

Spatially Resolved NMR Spectroscopy of Heterogeneous Gas Phase Hydrogenation of 1,3-Butadiene with Parahydrogen

Alexandra Svyatova,^{a,b} Elizaveta S. Kononenko,^{a,b} Kirill V. Kovtunov,^{*a,b} Dmitry Lebedev,^c Evgeniy Yu. Gerasimov,^{b,d} Andrey V. Bukhtiyarov,^{b,d} Igor P. Prosvirin,^{b,d} Valerii I. Bukhtiyarov,^d Christoph R. Müller,^e Alexey Fedorov^{*e} and Igor V. Koptiyug^{a,b,d}

^a International Tomography Center, SB RAS, 3 A Institutskaya st., Novosibirsk 630090, Russia. E-mail: kovtunov@tomo.nsc.ru

^b Novosibirsk State University, 2 Pirogova st., Novosibirsk 630090, Russia.

^c Department of Chemistry and Applied Biosciences, ETH Zürich, Vladimir-Prelog-Weg 1–5, Zürich CH 8093, Switzerland

^d Borekov Institute of Catalysis SB RAS, 5 Lavrenteva Pr., Novosibirsk 630090, Russia

^e Prof. C. R. Müller, Dr. A. Fedorov, Department of Mechanical and Process Engineering, ETH Zürich, Leonhardstrasse 21, Zürich CH 8092, Switzerland. E-mail: fedoroal@ethz.ch

Table of Contents

Preparation of the Reactors	2
Transmission Electron Microscopy Characterization	3
X-Ray Photoelectron Spectroscopy Characterization	4
Signal-to-noise Ratio (SNR) of NMR Spectra Obtained during 1,3-Butadiene Hydrogenation	5
MRI Experiments with <i>n</i>-H₂	6
MRI experiments with the presence of Teflon tube	6
MRI experiments with increased contact time	6
References	7

Preparation of the Reactors

Hydroxypropyl cellulose (HPC, Sigma Aldrich, average Mw approximately 80 kDa, 20 mesh), SiO_2 (Evonik Aerosol 200), Al_2O_3 (Evonik Aeroxide Alu 130), TiO_2 (Degussa Aeroxide P25), CeO_2 (Fluka AG), chloro-1,5-cyclooctadiene iridium dimer (Strem, 99%), chloro-1,5-cyclooctadiene rhodium dimer (Strem, 98%), tris(dibenzylideneacetone)dipalladium (Strem) and tris(dibenzylideneacetone)platinum(0) (Strem, 98%) were used to prepare porous reactive coatings on glass tube reactors decorated with metallic nanoparticles.

HPC (218 mg) was dissolved overnight in 2.5 mL of ethanol. Separately, the respective amount of an oxide (0.5 g of TiO_2 , 1 g of CeO_2 and 0.25 g of Al_2O_3 or SiO_2) was suspended in 2.5 mL of ethanol and combined with the HPC solution. The obtained paste was stirred for 2 hours followed by a 15 min sonication in an ultrasonic bath. The deposition of the paste on glass tubes (\varnothing 5 mm) was performed by drop casting of approximately 200 μL of the paste on the rotating tube (1000 rpm). Obtained samples were calcined for 1 hour at 500 $^\circ\text{C}$ and stored in air. Solutions of $[(\text{COD})\text{RhCl}]_2$ and $[(\text{COD})\text{IrCl}]_2$ were deposited from acetonitrile and solutions of $\text{Pd}_2(\text{dba})_3$ and $\text{Pt}(\text{dba})_3$ from acetonitrile : dichloromethane (1:1) mixture (27.5 μM). Solutions were deposited manually to produce arbitrary patterns of the oxide films deposited on glass tubes using a micropipette in air, using optimal amounts of the metal determined previously.¹ Overall, 16 reactors were tested in the hydrogenation reaction of 1,3-butadiene. The reactors contained nanoparticles of Rh, Ir, Pt, and Pd, supported on TiO_2 , CeO_2 , Al_2O_3 or SiO_2 .



Figure S1. Photographs of reactors with catalytic coatings (16 compositions) after heterogeneous catalytic hydrogenations of 1,3-butadiene.

Transmission Electron Microscopy Characterization

The support-glass interface was studied for all 4 oxide coatings using a scanning electron microscope JSM-6460 LV (Jeol, Japan). The images were obtained using secondary electrons (SE) at beam energy 20 keV.

TEM characterization of the catalytic coatings (Ir, Rh, Pd and Pt) was performed using silica as a representative support after the reduction in H_2 but before any catalytic tests. The images were collected using a JEM 2010 electron microscope (JEOL, Japan) with an accelerating voltage of 200 kV and line to line resolution of 0.14 nm.

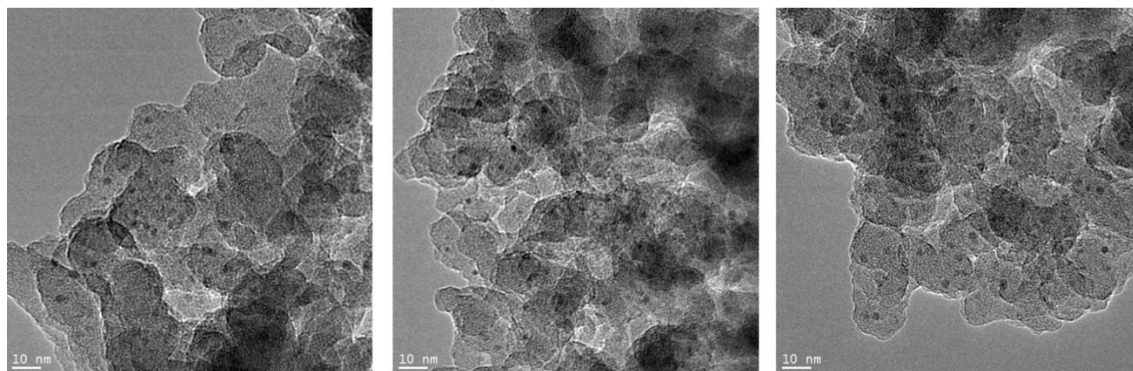


Figure S2. Representative TEM images of the Ir/SiO₂ reactive coating.

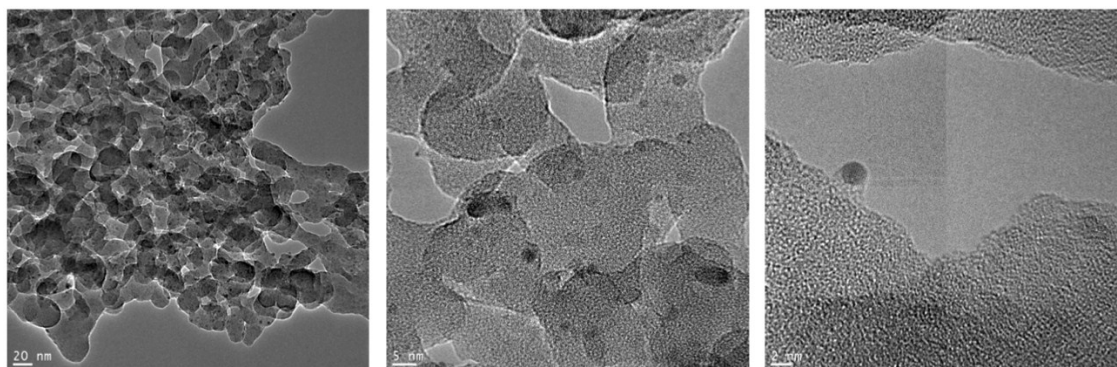


Figure S3. Representative TEM images of the Rh/SiO₂ reactive coating.

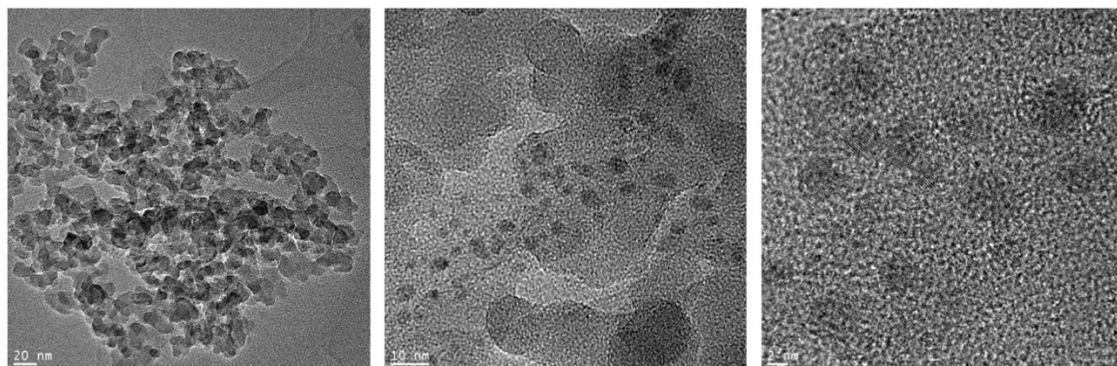


Figure S4. Representative TEM images of the Pd/SiO₂ reactive coating.

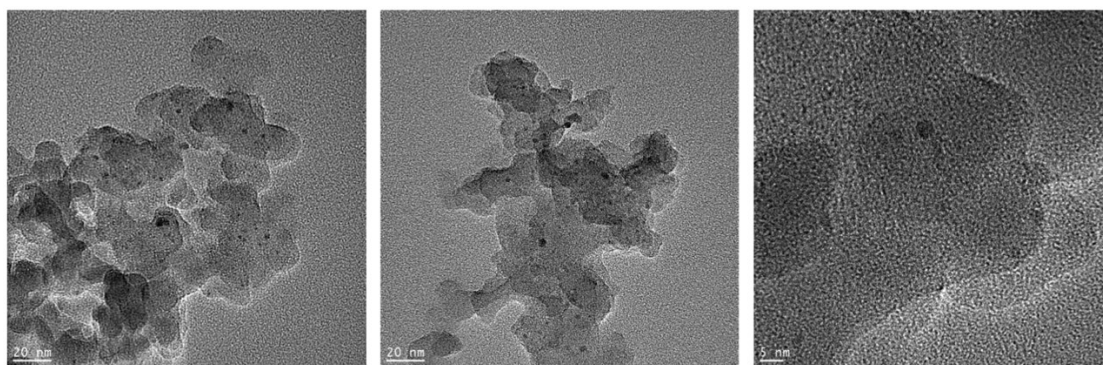


Figure S5. Representative TEM images of the Pt/SiO₂ reactive coating.

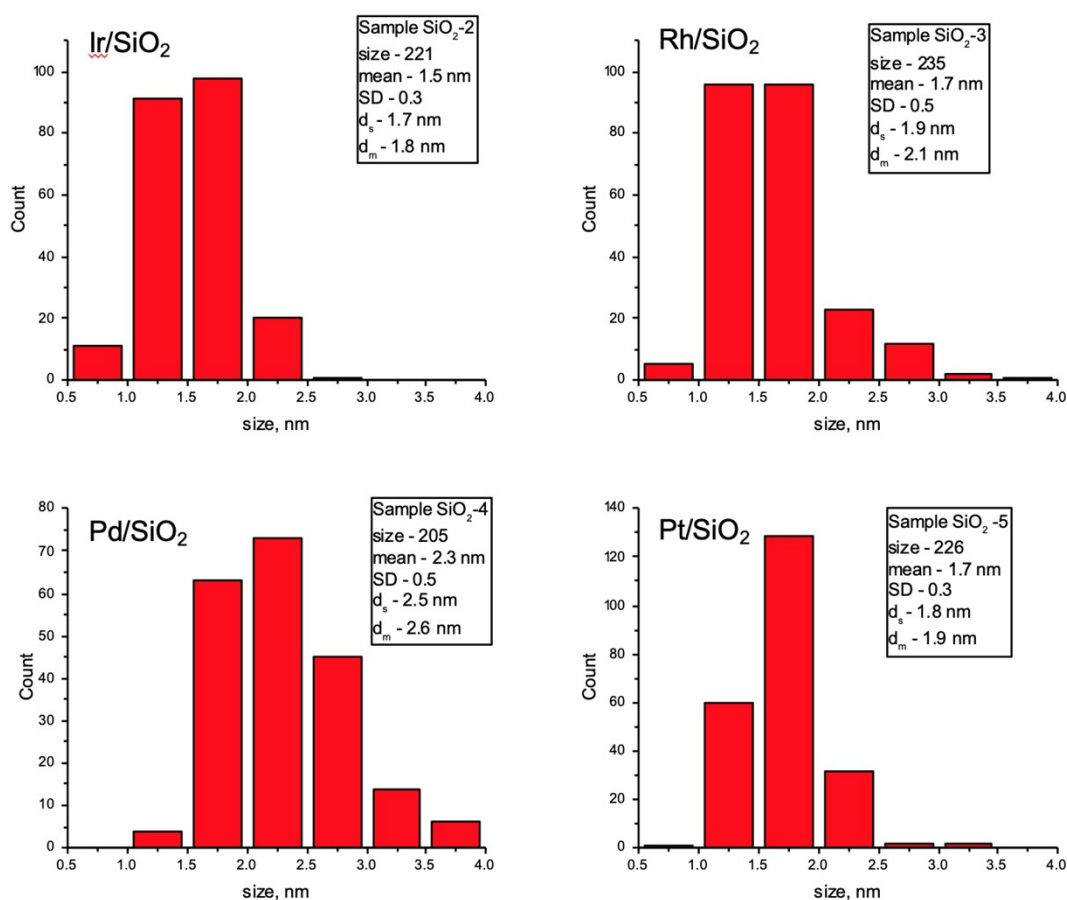


Figure S6. Particle size distribution of the respective reactive coatings.

X-Ray Photoelectron Spectroscopy Characterization

The XPS experiments were performed on a SPECS spectrometer equipped with a PHOIBOS-150 hemispherical energy analyzer and the X-Ray source with double Al/Mg anode. In the present work the AlK α ($h\nu = 1486.6$ eV, 200 W) was used as a primary irradiation. The binding energy (BE) scale was pre-calibrated using positions of Au4f_{7/2} (BE = 84.0 eV) and Cu2p_{3/2} (BE = 932.67 eV) core level peaks. The samples were supported onto double-sided conducting copper scotch tape. For the survey the pass energy of the analyzer of 50 eV was used and for the narrow spectral regions it was 20 eV. The atomic ratios of elements on the catalyst surface were calculated from the integral photoelectron peak intensities which were corrected with theoretical sensitivity factors based on Scofield's photoionization cross sections.² The binding energy was calibrated by position of the Al2p peak (BE = 74.5 eV), Si2p peak (BE = 103.3 eV), Ti2p_{3/2} peak (BE = 458.8 eV) and Ce3d (BE = 916.7 eV) corresponding to Al³⁺ in Al₂O₃, Si⁴⁺ in SiO₂, Ti⁴⁺ in TiO₂ and Ce⁴⁺ in CeO₂, respectively.³ Spectra analysis and peak fitting were performed with XPSPeak 4.1 software.⁴ Analysis of BE and shapes of photoelectron spectra of active components

(Ir4f, Pt4f and Pt4d, Rh3d, Pd3d) has shown the presence of two states for all samples: metallic and oxidized. For Ir supported samples the Ir4f_{7/2} BE are 60.7±0.1 and 61.9±0.1 eV, respectively.^{5,6} For Pd supported samples the Pd3d_{5/2} BE are 335.1±0.2 and 336.5±0.2 eV, respectively.⁷⁻⁹ For Pt supported samples the Pt4f_{7/2} BE are 71.3±0.2 and 72.5±0.2 eV, respectively.¹⁰⁻¹² For Rh supported samples the Rh 3d_{5/2} BE are 306.9±0.2 and 308.5±0.2 eV, respectively.^{13,14}

Table S2 shows the metal/support atomic ratios calculated from XPS spectra.

Table S1. Metal/support atomic ratios calculated from the XPS data.

Support	Description	Coating			
		Ir	Rh	Pd	Pt
Al ₂ O ₃	Before reaction	Ir/Al = 0.015	Rh/Al = 0.015	Pd/Al = 0.0	Pt/Al = 0.002
Al ₂ O ₃	After reaction	Ir/Al = 0.008	Rh/Al = 0.011	Pd/Al = 0.002	Pt/Al = 0.001
SiO ₂	Before reaction	Ir/Si = 0.003	Rh/Si = 0.004	Pd/Si = 0.006	Pt/Si = 0.003
SiO ₂	After reaction	Ir/Si = 0.007	Rh/Si = 0.006	Pd/Si = 0.003	Pt/Si = 0.005
CeO ₂	Before reaction	Ir/Ce = 0.04	Rh/Ce = 0.44	Pd/Ce = 0.03	Pt/Ce = 0.03
CeO ₂	After reaction	Ir/Ce = 0.06	Rh/Ce = 0.21	Pd/Ce = 0.026	Pt/Ce = 0.02
TiO ₂	Before reaction	Ir/Ti = 0.065	Rh/Ti = 0.05	Pd/Ti = 0.004	Pt/Ti = 0.006
TiO ₂	After reaction	Ir/Ti = 0.07	Rh/Ti = 0.03	Pd/Ti = 0.012	Pt/Ti = 0.005

Signal-to-noise Ratio (SNR) of NMR Spectra Obtained during 1,3-Butadiene Hydrogenation

SNRs were calculated by dividing the highest signal of the reaction product by the noise level defined using TopSpin.

Table S2. SNR of the different catalysts.

		COATING			
NANOPARTICLE		CeO ₂	SiO ₂	TiO ₂	Al ₂ O ₃
	Ir	186	220	128	103
	Rh	302	180	115	94
	Pd	86	26	290	122
	Pt	8	30	5	26

MRI Experiments with n-H₂

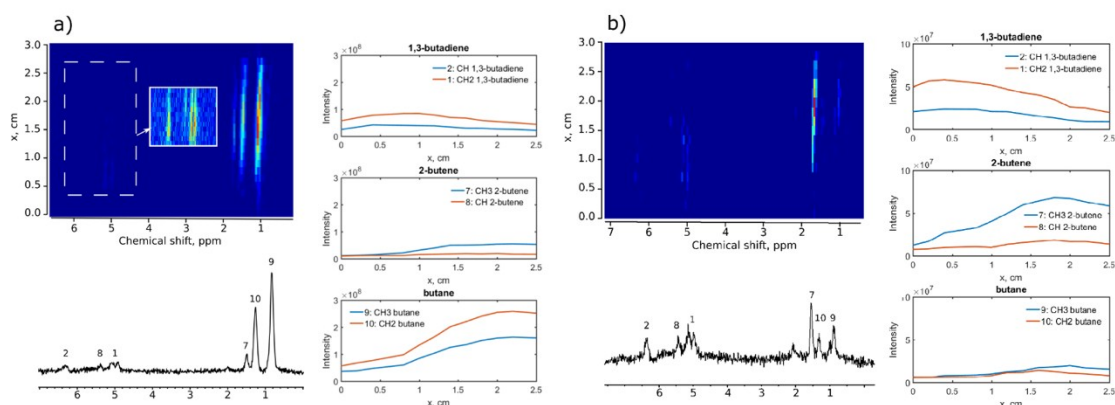


Figure S7. Hydrogenation of 1,3-butadiene over a) Ir/SiO₂ and b) Rh/CeO₂ catalysts with normal hydrogen (1,3-butadiene : H₂ ratio = 1:4, 5.1 mL s⁻¹ flow rate, 130 °C) as followed by MRI. Top panels: distribution of intensities of MRI signals in the working reactor along its length. Bottom panels: NMR spectra obtained during hydrogenation of 1,3-butadiene at high field of the spectrometer. Right panel: plots of distribution of the reaction products along the length of the reactor.

MRI experiments with the presence of Teflon tube

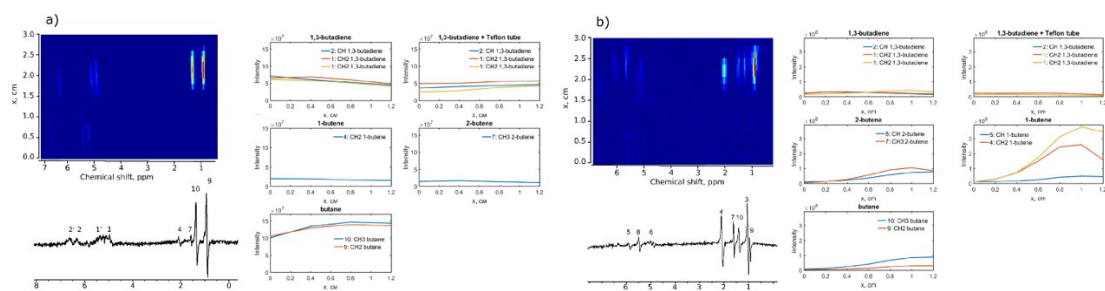


Figure S8. MRI experiments with a) Ir/SiO₂ and b) Rh/CeO₂ catalysts in 1,3-butadiene hydrogenation with parahydrogen with the Teflon tube hydrogen (1,3-butadiene : p-H₂ ratio = 1:4, 3.8 mL s⁻¹ flow rate, 130 °C). Top panels: distribution of intensities of MRI signals in the working reactor along its length. Bottom panels: NMR spectra obtained in PASADENA conditions. Chemical shifts marked with the prime correspond to NMR signals of 1,3-butadiene in the area with the Teflon tube. Right panel: plots of distribution of the reaction products along the length of the reactor.

MRI experiments with increased contact time

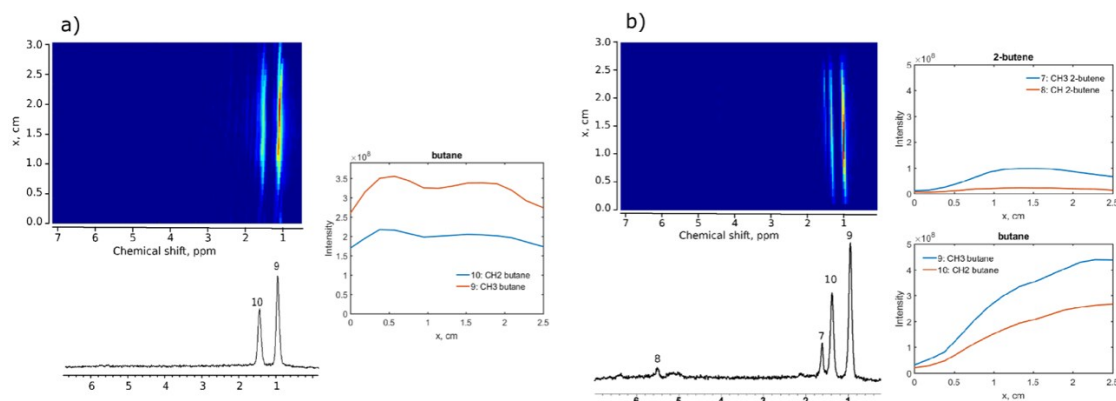


Figure S9. MRI experiments with a) Ir/SiO₂ and b) Rh/CeO₂ catalysts in 1,3-butadiene hydrogenation (1,3-butadiene : p-H₂ (or n-H₂) ratio = 1:4, 1.3 mL s⁻¹ flow rate, 130 °C) with p-H₂ and n-H₂, respectively. Top panel: MRI of the products distribution along the reactor length. Bottom panel: NMR spectrum obtained during hydrogenation of 1,3-butadiene at high field of the spectrometer. Right panel: distribution of the reaction products along the NMR tube.

References

1. K. V. Kovtunov, D. Lebedev, A. Svyatova, E. V. Pokochueva, I. P. Prosvirin, E. Y. Gerasimov, V. I. Bukhtiyarov, C. R. Müller, A. Fedorov and I. V. Koptug, *ChemCatChem*, 2019, **11**, 969–973.
2. J.H. Scofield. *J. Electron Spectrosc.*, 1976, **8**, 129–137.
3. J. F. Moulder, W. F. Stickle, P. E. Sobol and K. D. Bomben. Perkin-Elmer, Eden Prairie. MN, 1992, 261.
4. <http://xpspeak.software.informer.com/4.1/>
5. D. Labou, E. Slavcheva, U. Schnakenberg and S. Neophytides. *J. Power Sources*, 2008, **185**, 1073–1078.
6. F. Holsboer, W. Beck and H.D. Bartunik. *J.C.S. Dalton Trans.*, 1973, **17**, 1828–1829.
7. M. Brun, A. Berthet and J.C. Bertolini, *J. Electron Spectrosc.*, 1999, **104**, 55.
8. M. Peuckert. *J. Phys. Chem.*, 1985, **89**, 2481–2486.
9. Th. Pillo, R. Zimmermann, P. Steiner and S. Hufner. *J. Phys. Condens. Matter.*, 1997, **9**, 3987–3999.
10. M.-R. Gao, Z.-Y. Lin, J. Jiang, C.-H. Cui, Y.-R. Zheng and S.-H. Yu. *Chem. Eur. J.*, 2012, **18**, 8423–8429.
11. J.L.G. Fierro, J.M. Palacios and F. Tomas. *Surf. Interface Anal.*, 1988, **13**, 25–32.
12. G.C. Allen, Ph.M. Tucker, A. Capon and R. Parsons. *J. Electroanal. Chem. Interfacial Electrochem.*, 1974, **50**, 335–343.
13. Y.V. Larichev, O.V. Netskina, O.V. Komova and V.I. Simagina. *Int. J. Hydrog. Energy*, 2010, **35**, 6501–6507.
14. H. Guan, J. Lin, L. Li, X. Wang and T. Zhang. *Appl. Catal. B: Environm.*, 2016, **184**, 299–308.

Alexandra Svyatova, Elizaveta S. Kononenko, Kirill V. Kovtunov, Dmitry Lebedev, Evgeniy Yu. Gerasimov, Andrey V. Bukhtiyarov, Igor P. Prosvirin, Valerii I. Bukhtiyarov, Christoph R. Müller, Alexey Fedorov and Igor V. Koptug

K.V.K. and A.F. designed research; K.V.K., A.S., E.S.K. performed NMR and MRI measurements and analyzed the respective data; D.L. and A.F. prepared reactors with reactive coatings; I.P.P. and A.V.B. performed XPS analysis; E.Y.G. performed TEM analysis; K.V.K. and A.F. wrote the paper with contribution from all authors.